J Neurophysiol 115: 2635–2648, 2016.
First published February 10, 2016; doi:10.1152/jn.00816.2015.

Nicotine inhibits potassium currents in *Aplysia* bag cell neurons

Sean H. White, Raymond M. Sturgeon, and Neil S. Magoski
Department of Biomedical and Molecular Sciences, Physiology Graduate Program, Queen's University, Kingston, Ontario, Canada

Submitted 20 August 2015; accepted in final form 9 February 2016

White SH, Sturgeon RM, Magoski NS. Nicotine inhibits potassium currents in *Aplysia* bag cell neurons. *J Neurophysiol* 115: 2635–2648, 2016. First published February 10, 2016; doi:10.1152/jn.00816.2015.—Acetylcholine and the archetypal cholinergic agonist, nicotine, are typically associated with the opening of ionotropic receptors. In the bag cell neurons, which govern the reproductive behavior of the marine snail, *Aplysia californica*, there are two cholinergic responses: a relatively large acetylcholine-induced current and a relatively small nicotine-induced current. Both currents are readily apparent at resting membrane potential and result from the opening of distinct ionotropic receptors. We now report a separate current response elicited by applying nicotine to cultured bag cell neurons under whole cell voltage-clamp. This current was ostensibly inward, best resolved at depolarized voltages, presented a noncooperative dose-response with a half-maximal concentration near 1.5 mM, and associated with a decrease in membrane conductance. The unique nicotine-evoked response was not altered by intracellular perfusion with the G protein blocker GDPβS or exposure to classical nicotinic antagonists but was occluded by replacing intracellular K^+ with Cs^+. Consistent with an underlying mechanism of direct inhibition of one or more K^+ channels, nicotine was found to rapidly reduce the fast-inactivating A-type K^+ current as well as both components of the delayed-rectifier K^+ current. Finally, nicotine increased bag cell neuron excitability, which manifested as reduction in spike threshold, greater action potential height and width, and markedly more spiking to continuous depolarizing current injection. In contrast to conventional transient activation of nicotinic ionotropic receptors, block of K^+ channels could represent a nonstandard means for nicotine to profoundly alter the electrical properties of neurons over prolonged periods of time.

nicotine; inward current; K^+ channel block; excitability; mollusc

A PRIMARY DETERMINANT OF NEURONAL excitability is both the influence of leak K^+ channels on the resting membrane potential (Mathie et al. 2010) and the ability of voltage-gated K^+ channels to alter responsiveness or action potential dynamics (Johnston et al. 2010). Examples of this include serotonin acting through 5-HT_{apAC1} receptors to close S-type K^+ channels in *Aplysia* sensory neurons (Lee et al. 2009; Shuster et al. 1985; Siegelbaum et al. 1982), acetylcholine triggering M1 muscarinic receptors to shut M-type/K_V7 K^+ channels in vertebrate sympathetic neurons (Brown and Adams 1980; Marrion et al. 1989), or dopamine binding to D1-type receptors to reduce K_V1 K^+ channels in rat pyramidal neurons (Yang et al. 2013). Such decreases in K^+ current can influence both sensitivity and the transition to persistent firing. A neuron that continuously spikes typically presents a region of negative slope in the steady-state current-voltage (*I/V*) relationship (Wilson and Wachtel 1974). Whereas opening of inward currents, such as nonselective cation channels (Inoue and Kuriyama 1991; Partridge et al. 1979; Wilson et al. 1996) or persistent Ca^{2+} channels (Carlin et al. 2000; Eckert and Lux 1976; Lee and Heckman 1998), is often responsible for negative slope, it also can be brought about by lowering outward K^+ channels (Beilby 1986; Lüthi et al. 1997; Shen and Johnson 2013). In this study, we show that block of K^+ currents by nicotine can produce negative slope in molluscan neuroendocrine cells.

For the anaspidean marine snail, *Aplysia californica*, reproductive behavior is initiated by the bag cell neurons (Conn and Kaczmarek 1989; Kupfermann et al. 1966; Kupfermann and Kandel 1970; Zhang and Kaczmarek 2008). Located in two clusters at the rostral end of the abdominal ganglion, these neuroendocrine cells cause ovulation through the neurohemal release of egg-laying hormone (Arch 1972; Coggeshall 1967; Ferguson et al. 1989; Frazier et al. 1967). Secretion occurs when the neurons shift from quiescence to a state of constant firing, termed the afterdischarge, that lasts ~30 min (Kaczmarek et al. 1982; Loechner et al. 1990; Michel and Wayne 2002). Bag cell neuron excitability is strongly influenced by K^+ channels; for example, in juvenile animals, the neurons fail to afterdischarge, mainly due to elevated K^+ currents (Nick et al. 1996b). Conversely, reducing overall K^+ current by block with tetraethylammonium (TEA) either increases the likelihood of an afterdischarge upon synaptic stimulation or induces an afterdischarge de novo (Kaczmarek et al. 1982; Nick et al. 1996a). The main voltage-gated K^+ channels in these neurons include a fast-activating A-current and a two-component delayed-rectifier current, all of which are inhibited near the start of the afterdischarge by kinase-dependent phosphorylation (Jennings et al. 1982; Kaczmarek and Strumwasser 1984; Strong 1984; Strong and Kaczmarek 1986).

Although the afterdischarge is lengthy in duration, it is triggered by brief cholinergic afferent input and can be mimicked by exogenous acetylcholine application (White and Magoski 2012). Acetylcholine generates an inward current through opening of a ionotropic receptor that passes monovalent cations. Interestingly, nicotine also causes inward current, but through activation of a second ligand-gated channel, with pharmacology and cationic selectivity distinct from the acetylcholine receptor (White et al. 2014). The present study demonstrates that nicotine can elicit an apparent inward current, but in this instance by inhibiting outward K^+ channels. This response appears at depolarized potentials following nicotine application, is associated with a decrease in conductance, and profoundly enhances excitability. Thus nicotine may act as a true K^+ channel blocker, which has implications for both chronic nicotine exposure and signaling via noncanonical cholinergic pathways.

Address for reprint requests and other correspondence: N. S. Magoski, Queen's Univ., Dept. of Biomedical and Molecular Sciences, 4th Floor, Botterell Hall, 18 Stuart St., Kingston, ON, Canada K7L 3N6 (e-mail: magoski@queensu.ca).

MATERIALS AND METHODS

Animals and cell culture. Adult *A. californica* weighing 150–500 g were obtained from Marinus (Long Beach, CA), housed in an ~300-liter aquarium containing continuously circulating aerated artificial sea water (Instant Ocean; Aquarium Systems, Mentor, OH) at 15°C on a 12:12-h light-dark cycle, and fed Romaine lettuce 5 times per week. All experiments were approved by the Queen's University Animal Care Committee (protocols Magoski-2009-065 or Magoski-2013-041).

For primary cultures of isolated bag cell neurons, animals were anesthetized by an injection of isotonic $MgCl_2$ (~50% body wt), and the abdominal ganglion was removed and treated with neutral protease (13.33 mg/ml; 165859; Roche Diagnostics, Indianapolis, IN) dissolved in tissue culture artificial sea water (tcASW; composition in mM: 460 NaCl, 10.4 KCl, 11 $CaCl_2$, 55 $MgCl_2$, 15 HEPES, 1 mg/ml glucose, 100 U/ml penicillin, and 0.1 mg/ml streptomycin; pH 7.8 with NaOH) for 18 h at 20–22°C. The ganglion was then transferred to fresh tcASW for 1 h, after which the bag cell neuron clusters were dissected from their surrounding connective tissue, and with the use of a fire-polished Pasteur pipette for gentle trituration, neurons were dispersed in tcASW onto 35- × 10-mm polystyrene tissue culture dishes (430165; Corning, Corning, NY; or 353001; Falcon Becton-Dickinson, Franklin Lakes, NJ). Cultures were maintained in tcASW in a 14°C incubator and used for voltage- or current-clamp experiments (see below) within 1–3 days. Data were collected at room temperature (20–22°C). Salts were obtained from Fisher Scientific (Ottawa, ON, Canada), ICN (Aurora, OH), or Sigma-Aldrich (St. Louis, MO).

Whole cell voltage-clamp recording. Voltage-clamp recordings were made using an EPC-8 amplifier (HEKA Electronics; Mahone Bay, NS, Canada) and the tight-seal whole cell method. Microelectrodes were pulled from 1.5-mm external, 1.2-mm internal diameter borosilicate glass capillaries (TW150F-4; World Precision Instruments, Sarasota, FL) and had a resistance of 1–2 MΩ when fire-polished and filled with intracellular saline (see below). Before seal formation, pipette junction potentials were nulled. After seal formation, the pipette capacitive current was canceled, and after breakthrough, the whole cell capacitive current was canceled, while the series resistance (3–5 MΩ) was compensated to 80% and monitored throughout the experiment. Data were acquired using the Clampex program of the pCLAMP suite (v10.0; Molecular Devices, Sunnyvale, CA), a Digidata 1322A analog-to-digital converter (Molecular Devices), and an IBM-compatible personal computer. Current was filtered at 1 kHz with the EPC-8 Bessel filter and sampled at 2 kHz.

Initial recordings were made in normal artificial seawater (nASW; composition as per tcASW but lacking glucose and antibiotics) with standard intracellular saline [composition in mM: 500 K^+-aspartate, 70 KCl, 1.25 $MgCl_2$, 10 HEPES, 11 glucose, 10 glutathione, 5 EGTA, 5 adenosine 5′-triphosphate disodium salt hydrate (A3377; Sigma-Aldrich), and 0.1 guanosine 5′-triphosphate sodium salt hydrate (GTP; G8877; Sigma-Aldrich); pH 7.3 with KOH] in the recording pipette. The free intracellular Ca^{2+} concentration was set at 300 nM by adding 3.75 mM of $CaCl_2$, as calculated by WebMaxC (http://www.stanford.edu/~cpatton/webmaxcS.htm). In some instances, K^+ was replaced with Cs^+ or GTP replaced with 10 mM guanosine 5′-(β-thio)diphosphate trilithium salt (GDPβS; G7637; Sigma-Aldrich). For isolation of K^+ currents, Na^+-free/Ca^{2+}-free ASW was used as the external solution, with Na^+ replaced by *N*-methyl-D-glucamine ($NMDG^+$) and Ca^{2+} replaced by Mg^{2+}. As necessary, online leak subtraction employed a P/4 protocol with subpulses of opposite polarity and one-quarter the magnitude of each test pulse (Bezanilla and Armstrong 1977). The inter-subpulse interval was 500 ms, with 5–10 s between test pulses. Junction potentials of 15 and 23 mV were calculated for the intracellular saline vs. nASW and Na^+-free/Ca^{2+}-free ASW, respectively; both were subtracted off-line.

Sharp-electrode current-clamp recording. Current-clamp recordings were made in nASW using an AxoClamp 2B amplifier (Molecular Devices) and the sharp-electrode bridge-balanced method. Microelectrodes were pulled from 1.2-mm external, 0.9-mm internal diameter borosilicate glass capillaries (TW120F-4; World Precision Instruments) and had a resistance of 5–20 MΩ when filled with 2 M K^+-acetate, 10 mM HEPES, and 100 mM KCl (pH 7.3 with KOH). When necessary, neurons were set to −60 mV using the AxoClamp DC current command while Clampex was used to inject step current. Voltage was filtered at 3 kHz, using the AxoClamp Bessel filter, and sampled at 2 kHz as in *Whole cell voltage-clamp recording*.

Drug application and reagents. The culture dish served as the bath. For single-cell microperfusion, i.e., superfusion, a micromanipulator-controlled square-barrel glass pipette (~500-μm bore) was positioned 300–500 μm from the soma and connected by a stopcock manifold to a series of gravity-driven reservoirs. This provided a constant flow (0.5–1 ml/min) of control extracellular saline over the neuron, which was switched to saline containing nicotine for a specific amount of time by activating the appropriate stopcock. Nicotine was also pressure-ejected from an unpolished patch pipette (1- to 2-μm bore) for 2 s at 75–150 kPa using a PMI-100 pressure microinjector (Dagan, Minneapolis, MN). To access the pharmacology of the nicotine-evoked response, antagonists were delivered directly to the bath between successive pressure applications, separated by ~10 min. As previously undertaken with bag cell neurons by Fisher et al. (1993) and ourselves (White and Magoski 2012), perfusion was typically not employed during pressure application; however, the pipette was removed from the bath immediately after each ejection to minimize leakage and possible desensitization. In some experiments, nASW, nicotine, or the structurally similar agonist, epibatidine (Badio and Daly 1994), was continuously pressured-applied for 10 s.

Drugs were made up as stock solutions in water, frozen at −20°C, and then diluted down to a working concentration in the extracellular or intracellular solutions as needed: nicotine (N0257; Sigma-Aldrich), mecamylamine hydrochloride (M9020; Sigma-Aldrich), α-conotoxin ImI (3119; Tocris Bioscience), hexamethonium dichloride (H2138; Sigma-Aldrich), (±)-epibatidine dihydrochloride hydrate (E1145; Sigma-Aldrich).

Analysis. The Clampfit program of pCLAMP was used to determine the amplitude and time course of changes to ligand- or voltage-gated current as well as the membrane potential or action potentials. For changes to steady-state current or membrane potential, after 1 min of baseline, two cursors were placed immediately before the current or voltage change while an additional two cursors were positioned to encompass the peak response. Clampfit then calculated the average current or voltage between the cursor pairs. The maximal response was taken as the difference between the average baseline and peak values. Similar measurements were made for voltage-dependent current, which in most cases was then normalized to cell size by dividing by the whole cell capacitance (as determined by the EPC-8 slow capacitance compensation circuitry). The peak and time to peak of the action potential were determined using Clampfit by setting cursors immediately before the spike and along the falling phase. The action potential half-width was found by taking the time from the peak to halfway down the falling phase between the peak and the trough. Conductance was derived using Ohm's law ($G = I/V$) from the current during a 1-s step from 0 to −10 mV. In cases where nicotine was applied twice, the subsequent application occurred after an ~10-min interval, and any change in peak current was quantified by expressing the second response as a percentage of the first. For display, some nicotine-evoked current traces were filtered off-line to between 20 and 80 Hz using the Clampfit Gaussian filter; comparison with original data ensured that this second filtering brought about no change in amplitude or kinetics. The concentration-response curve was fitted with a Hill slope equation:

$$Y = \text{bottom} + \left(\text{top} - \text{bottom}\right) / \left[1 + 10^{\left(\log e_{50} - X\right) \cdot \text{Hill slope}}\right]$$

using Prism (v5.04; GraphPad Software, La Jolla, CA) and the least-squares method, where bottom is the basal response, top is the

maximal response, and EC_{50} is the 50% effective concentration. The fast and slow time constants (τ_1 and τ_2) of the delayed-rectifier K^+ currents were determined by fitting tail currents with a standard two-term exponential:

$$f(t) = \sum_{i=1}^{n=2} A_i e^{-t/\tau_i} + C$$

using Clampfit and the Chebyshev method, where i is the index of summation, n is the upper bound of summation, A is the amplitude, τ is the time constant, and C is the constant y-offset. The same equation was also used to fit delayed-rectifier K^+ current use-dependent inactivation plots.

Statistical analysis was performed using Prism. The Kolmogorov-Smirnov method was used to test data sets for normality. To test whether the mean differed between two groups, either Student's paired or unpaired t-test (for normally distributed data) with the Welch correction as necessary (for unequal standard deviations) or the Mann-Whitney U-test (for not normally distributed data) was used. Comparing more than two means involved a one-way ordinary or repeated-measures analysis of variance (ANOVA), followed by the Dunnett multiple comparisons test. Means were considered significantly different if the two-tailed P value was <0.05. Data are means ± SE.

RESULTS

While characterizing the more orthodox, linear inward current induced by nicotine at −60 mV (see White et al. 2014 for details), we noticed an apparent voltage-dependent current, which began at approximately −30 mV and then increased in magnitude with further depolarization. This was similar to the inverted U-shaped *I/V* relationship caused by nicotine in dorsal unpaired median cells of the cockroach, *Periplanta* (Courjaret and Lapied 2001; Thany et al. 2008). That result was attributed to an atypical nicotinic receptor that closed upon agonist binding. Thus we sought to determine if the nicotine-evoked current at depolarized potentials was receptor mediated or, as reported in rat heart (Wang et al. 2000a, 2000b), due to nicotine in some way blocking K^+ channels.

Nicotine produces negative slope in the I/V relationship of bag cell neurons. Cultured bag cell neurons were whole cell voltage-clamped in nASW and perfused intracellularly for at least 5 min with our standard K^+-aspartate-based intracellular solution via the recording pipette (see MATERIALS AND METHODS, *Whole cell voltage-clamp recording*). To examine if current changed in a voltage-dependent manner during nicotine superfusion, a 10-s voltage ramp from −90 to +20 mV was applied 4 times, with 2-min intervals between each ramp. The first and second ramp served as the control period, where nicotine was not applied. Subtracting the current evoked by the first ramp from that elicited by the second ramp provided a difference current with a relatively flat *I/V* relationship (Fig. 1*A*, black trace), although in some neurons we observed a small outward current at voltages more positive than −20 mV. Between the third and fourth ramp, 3 mM nicotine was continuously perfused over the same neuron, i.e., 2 min of nicotine. On the basis of our previous work, we know that this lengthy nicotine exposure would result in desensitization of any nicotinic ionotropic receptors that normally pass inward current at −60 mV (White et al. 2014). The difference current obtained by subtracting the current produced by the third ramp from that triggered by the fourth ramp (in nicotine) yielded a negative-slope *I/V* relationship that was inward and voltage dependent with an onset near −30 mV (Fig. 1*A*, gray trace).

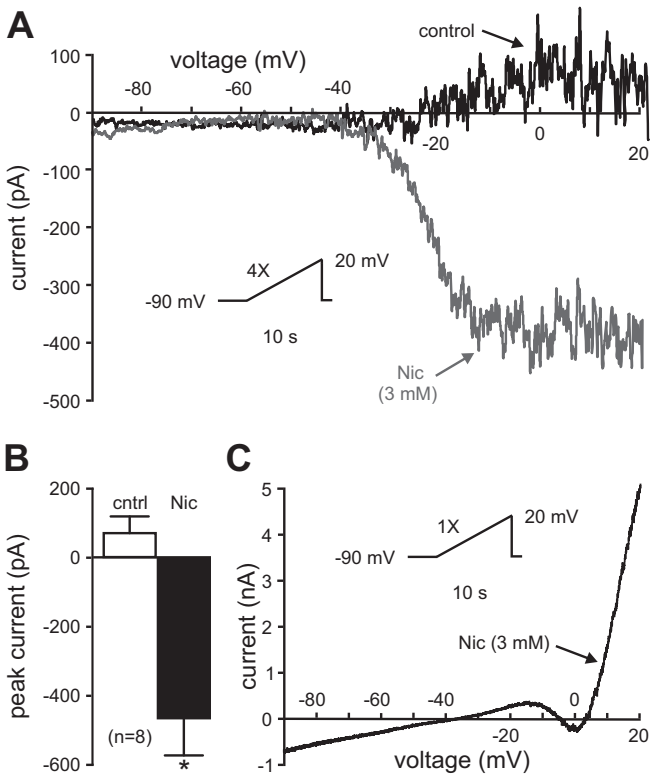

Fig. 1. Nicotine superfusion generates a voltage-dependent current in cultured bag cell neurons. *A*: subtraction currents taken from a whole cell voltage-clamp recording of a cultured bag cell neuron in nASW and perfused intracellularly with K^+-aspartate-based intracellular saline. A total of four 10-s ramps from −90 to +20 mV (*inset*) were given, each separated by 2 min. In control conditions (black trace), before the addition of nicotine, subtracting the first ramp current from the second furnished an essentially flat *I/V* relationship, with only a small outward current at positive voltages. However, subtracting the third ramp current from the fourth [taken after the neuron was exposed to 3 mM nicotine (Nic) for the full 2 min] (gray trace) revealed an inward current characteristic of negative slope in the *I/V* relationship, i.e., developing at approximately −30 mV and peaking around 0 mV. *B*: summary data show a significantly greater peak current during the ramp in nicotine compared with the response before agonist application (*$P < 0.01$, paired Student's t-test). *C*: total membrane current elicited during the ramp while in the presence of nicotine. In this nonsubtracted *I/V* relationship, negative slope appears at about −10 mV, with a nadir close to 0 mV, before turning outward again. Recordings were taken from the same neurons summarized in *B*.

The subtraction current in nicotine reached maximal amplitude between −10 and 0 mV. On average, this corresponded to a peak of approximately −450 pA, which was significantly different from the approximately +50-pA current elicited by the ramp under control conditions ($n = 8$; Fig. 1*B*). With respect to total membrane current, Fig. 1*C* provides a nonsubtracted current trace, produced by the ramp, from one of the eight nicotine-exposed neurons. In this case, a negative slope was apparent in the total *I/V* relationship beginning at −10 mV, with a peak inward current around 0 mV.

A concentration-dependent, nicotine-evoked current at depolarized potentials. Our earlier study showed that nicotine induced an ionotropic inward current at −60 mV, which reversed at approximately −25 mV, but passed little outward current at voltages more positive than the reversal potential (White et al. 2014). Since this reversal potential overlaps with the development of the voltage-dependent current at approximately −30 mV, cultured bag cell neurons were whole cell

voltage-clamped to −10 mV, to isolate as much as possible the second type of nicotine-evoked response. To generate a concentration-response relationship, nicotine was superfused at concentrations ranging from 300 μM to 30 mM, for 30 s each, with 10 min between applications. Responses were repeatable, and up to three concentrations were delivered per neuron. Example traces during perfusion of 300 μM, 1 mM, 3 mM, or 10 mM nicotine are shown in Fig. 2*A*. Average current densities (peak current normalized to cell capacitance) from multiple concentrations yielded a curve with a peak of ~600 pA/pF, a Hill slope of 1.08, indicating lack of cooperative binding, and an EC_{50} of 1.38 mM (Fig. 2*B*). Based on these values, it appears that the current at −10 mV does not involve the same receptor as the current induced by nicotine at −60 mV, which was cooperative (Hill slope = 2.4) and left-shifted (EC_{50} = 240 μM) (White et al. 2014).

To test for a change in conductance during nicotine exposure, neurons were held at 0 mV and a 1-s step to −10 mV was applied (n = 9; Fig. 2*C*, *bottom*). Before the introduction of nicotine, under control conditions, the hyperpolarizing step produced an inward current of usually several hundred picoamperes (Fig. 2*C*, *top*, black trace). Delivering the pulse 2 min later, during the current induced by 3 mM nicotine (a concentration near the EC_{50}), resulted in a noticeably smaller step current (Fig. 2*C*, *top*, gray trace). On average, compared with the control conductance of ~35 nS, the conductance in the presence of nicotine was significantly smaller at ~27 nS (Fig. 2*D*). This suggested that the nicotine-evoked response at −10 mV was due to a channel closure, as opposed to our preceding work demonstrating channel opening by nicotine at −60 mV (White et al. 2014).

The nicotine-evoked response at −10 mV is dependent on K^+. An initial examination of the response to nicotine at holding potentials ranging from −10 to +60 mV revealed that the current increased in magnitude with more positive voltages (data not shown). The augmentation of inward current at more depolarized potentials was similar to the decrease-conductance K^+-dependent postsynaptic potential in *Aplysia* L14 ink motor neurons (Carew and Kandel 1977). Thus the response in cultured bag cell neurons may involve K^+ channel block, and we attempted to occlude this by replacing the K^+ in the whole cell pipette with Cs^+, a K^+ channel blocker (Adelman and Senft 1966; Hille 2001). During holding at −10 mV, a 1-min continuous perfusion of 3 mM nicotine led to a relatively large nondesensitizing current with K^+-based internal solution (n = 10; Fig. 3*A*, *top*); however, inclusion of Cs^+ in the pipette (n = 12) either decreased or eliminated the response entirely (Fig. 3*A*, *bottom*). The mean peak current density was ~0.1 pA/pF following intracellular Cs^+ perfusion, which was significantly different from the ~0.7 pA/pF with intracellular K^+ perfusion (Fig. 3*B*).

The nicotine-evoked response at −10 mV is not dependent on G proteins. There is a possibility that the nicotine response is due to a nicotinic receptor metabotropically closing ion channels. For example, Tieman et al. (2001) used both electrophysiology and chromatography to show that nicotine-gated ionotropic receptors can activate lipoxygenase via G proteins in neural tissue and identified neurons from *Aplysia*. As such,

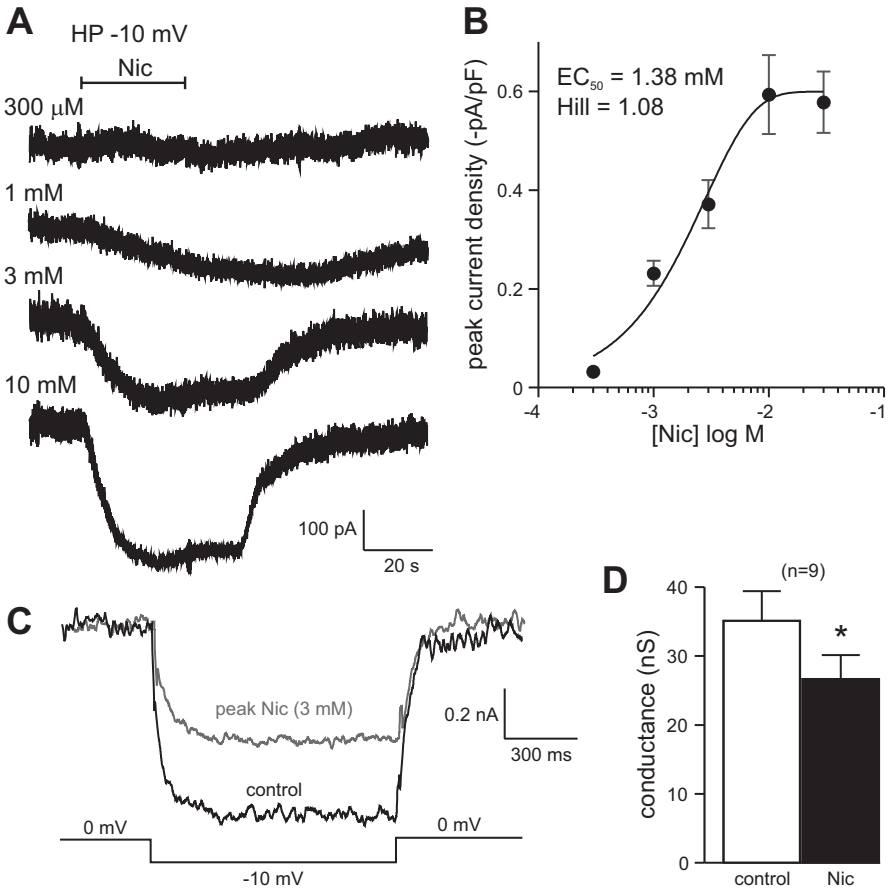

Fig. 2. Current responses to nicotine application at a depolarized voltage. *A*: a cultured bag cell neuron whole cell voltage-clamped in nASW with K^+-based internal solution. At a holding potential (HP) of −10 mV, microsuperfusion (at horizontal bar) of nicotine (Nic) for 30 s induced a current that grew both in magnitude and speed of onset as the concentration was increased from 300 μM through 10 mM. Scale bars apply to all traces. *B*: fitting the concentration-response curve for the peak change in current density following nicotine application revealed an EC_{50} of 1.38 mM and a noncooperative Hill coefficient of 1.08 (n = 6 for 300 μM, 7 for 1 mM, 9 for 3 mM, 12 for 10 mM, 3 for 30 mM). *C*: in a different neuron, membrane conductance was tested with a 1-s hyperpolarizing step from 0 to −10 mV under voltage clamp (*bottom*). In control, before nicotine application, the step current was approximately −700 pA (*top*, black trace). This was reduced to approximately −400 pA when the step was given at the peak of the response to 3 mM nicotine (*top*, gray trace). Traces are overlaid for clarity and display. Scale bars apply to both traces. *D*: the change in conductance, calculated from Ohm's law ($G = I/V$), was significantly reduced during nicotine compared with control (*$P < 0.05$, paired Student's t-test).

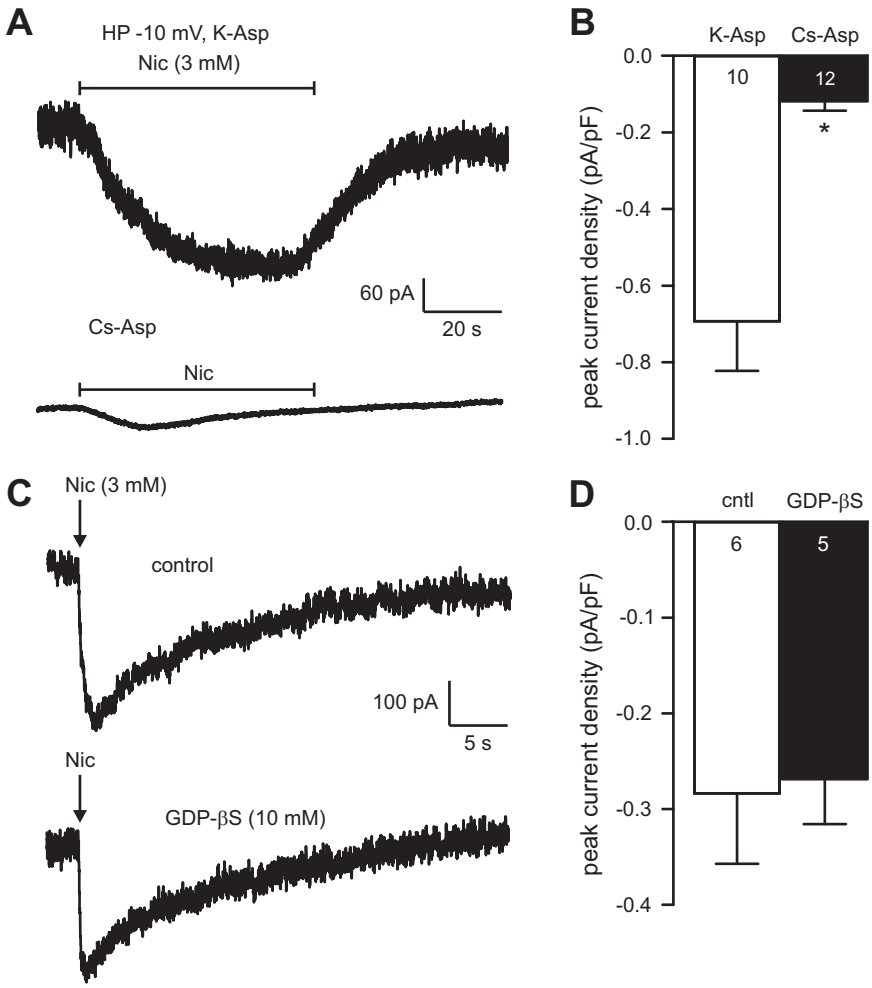

Fig. 3. The nicotine-evoked response at −10 mV is lost with intracellular Cs^+ perfusion and is not sensitive to a general G protein blocker. *A*, *top*: whole cell current following a 1-min superfusion (at horizontal bar) of 3 mM nicotine (Nic) in a cultured bag cell neuron voltage-clamped to a holding potential (HP) of −10 mV in nASW with K^+-based internal solution. *Bottom*, in a different neuron, the response to nicotine was largely abolished after 30-min intracellular perfusion with a Cs^+-based internal solution to block K^+ channels. Note the overall drop in baseline noise of the current is likely due to intracellular Cs^+ reducing those K^+ channels open at −10 mV. Prior work has shown intracellular Cs^+ blocks nearly all outward current from bag cell neurons (Groten and Magoski 2015; Strong and Kaczmarek 1986). Any remaining response to nicotine probably represents inhibition of residual K^+ current. Scale bars apply to both traces. *B*: summary data indicating a significantly reduced change in peak current following nicotine when K^+ was replaced with Cs^+ in the recording pipette (*$P < 0.01$, unpaired Student's *t*-test, Welch corrected). Numbers in bars indicate number of neurons. *C*: pressure application (at arrow) of 3 mM nicotine induced a current response at a HP of −10 mV following 30-min intracellular perfusion with K^+-based internal solution containing 0.1 mM GTP (*top*). This is similar to a separate neuron perfused for 30 min with the same internal solution, except for 10 mM GDPβS replacing GTP (*bottom*). Scale bars apply to both traces. *D*: the mean peak current density of the nicotine response with a GDPβS-containing internal solution is not significantly different compared with control (Mann-Whitney *U*-test). Numbers in bars indicate number of neurons.

cultured bag cell neurons were perfused intracellularly for 30 min with standard internal solution plus 10 mM GDPβS, a nonhydrolyzable GDP analog that inhibits heterotrimeric G proteins by competing with GTP for α-subunit binding (Eckstein et al. 1979). Compared with controls perfused intracellularly with GTP ($n = 6$; Fig. 3*C*, *top*), introducing GDPβS did not alter the response to 3 mM nicotine at −10 mV ($n = 5$; Fig. 3*C*, *bottom*). In these experiments, we employed a 2-s pressure application of nicotine, which we found as effective as perfusion in bringing about an effect. The summary data revealed no significant difference in the current density for GDPβS vs. GTP, with both at ~0.3 pA/pF (Fig. 3*D*). We previously showed that GDPβS eliminated an outward current in bag cell neurons induced by FMRFamide (White and Magoski 2012), which is known to act via metabotropic receptors in molluscs (Brezina et al. 1987; Piomelli et al. 1987a, 1987b). Additional work in our laboratory and elsewhere finds GDPβS to effectively prevent G protein-mediated currents or depolarizations in neurons from both *Aplysia* and the pulmonate mollusc, *Lymnaea* (Bolshakov et al. 1993; Kehoe 1994; Lemos and Levitan 1984; Magoski et al. 1995; Tam et al. 2011).

Pharmacology of the nicotine-evoked response at −10 mV. We next explored the prospect that the nicotine-evoked response at −10 mV involved a traditional nicotinic receptor. Nicotine was pressure-applied twice to whole cell voltage-clamped cultured bag cell neurons at −10 mV; applications were separated by a minimum of 10 min. Classical nicotinic antagonists were introduced directly into the bath after the first nicotine application, and their relative effectiveness determined by calculating the percent change in the peak current between the first and second nicotine responses (see MATERIALS AND METHODS, *Drug application and reagents* and *Analysis*). Under control conditions, without the addition of any antagonist to the bath, the second ejection of nicotine at −10 mV produced a response that was essentially equal to the first ($n = 10$; Fig. 4*A*, *top* vs. *bottom*, and *C*). A concentration of 100 μM mecamylamine (Ascher et al. 1979; Stone et al. 1956), which blocks the nicotine current at −60 mV (White et al. 2014), failed to alter the nicotine-evoked response at −10 mV and resulted in a similar percentage of remaining current as that of control, i.e., ~100% ($n = 5$; Fig. 4, *B* and *C*). Likewise, neither 1 μM α-conotoxin ImI ($n = 7$) (Ellison et al. 2003; McIntosh et al. 1994) nor 100 μM hexamethonium ($n = 6$) (Ascher et al. 1978; Kehoe 1972) altered the second nicotine-evoked response (Fig. 4*C*).

Short-term nicotine treatment inhibits voltage-gated K^+ currents. Thus far, our observations suggested that nicotine inhibits some form of K^+ current. We next examined whether a similar outcome occurs with the fast-inactivating A-type (I_A) and delayed-rectifier K^+ (I_K) currents. To isolate K^+ currents, we replaced the extracellular Na^+ and Ca^{2+} with $NMDG^+$ and Mg^{2+}, respectively, while using our standard K^+-aspartate-

based intracellular solution. The Na^+-free, Ca^{2+}-free ASW has been used by our laboratory and others to observe K^+ currents in bag cell neurons (Dargaei et al. 2014; Zhang et al. 2002). To record I_A, which requires hyperpolarization from resting potential to deinactivate, cultured neurons were voltage-clamped at a holding potential of −90 mV, followed by 500-ms voltage steps to −80, −60, −40, and −20 mV (Fig. 5*A*, *bottom*) (Strong 1984). I_K were studied by holding at −60 mV, which inactivates essentially all I_A, and then making 200-ms pulses to −40, −20, 0, +20, and +40 mV (Fig. 5*B*, *bottom*) (Strong and Kaczmarek 1986). For both currents, before each step, a P/4 protocol was used to subtract leak currents (see MATERIALS AND METHODS, *Whole cell voltage-clamp recording*). When possible, the same neuron was used to examine I_A and I_K, as well as tail currents for the isolation of the two components of I_K (see last paragraph of this section).

In control neurons (n = 11), I_A was first apparent during the 500-ms step to −60 mV from −90 mV, but was rapidly and completely inactivated to baseline by the end of the pulse (Fig. 5*A*, *top*). Similarly, steps to −40 and −20 mV also activated the current, albeit they were larger (peak ~30 pA/pF at +20 mV), had faster onset kinetics, and lacked complete inactivation over the duration of the stimulus. In separate neurons, where 10 mM nicotine was perfused for at least 10 min before recording (n = 11), both the peak and steady-state I_A were diminished (Fig. 5*A*, *middle*). When normalized to cell capacitance, the peak current density was significantly less in the presence of nicotine at both resting membrane potential (−60 mV) and moderately depolarized voltages (−40 and −20 mV) compared with controls (Fig. 5*C*). The blocking effect of nicotine appeared voltage dependent, based on a fourfold reduction at −20 mV compared with a twofold reduction at −40 mV.

A similar drop in peak current magnitude occurred with 10 mM nicotine exposure for I_K. In control neurons (n = 11), from a holding potential of −60 mV, very little current was evident without substantial depolarization, i.e., only during the 200-ms step to −20 mV did a relatively slowly activating K^+ current initially appear (Fig. 5*B*, *top*). However, current activation and magnitude was progressively accelerated with step depolarizations beyond −20 mV (peak ~35 pA/pF at +40 mV). By the end of the pulse, much of the sustained current was still present. Nicotine (n = 12) attenuated both the peak and sustained responses (Fig. 5*B*, *middle*), with the I_K peak current density being significantly reduced at all voltages from −20 to +40 mV (Fig. 5*D*). Contrary to the effect of nicotine on I_A, the block of I_K was not augmented by depolarization.

The actions of nicotine on both I_A and I_K were reversible. To demonstrate this, we compared each current before, during, and after 30 s of 10 mM nicotine perfusion (n = 7). Currents were evoked by holding neurons at specific voltages and stepping to only one potential (to −40 from −90 mV for I_A and to +30 from −60 mV for I_K). For I_A, the 500-ms step to −40 mV (Fig. 5*E*, *bottom*) produced a typical fast-activat-

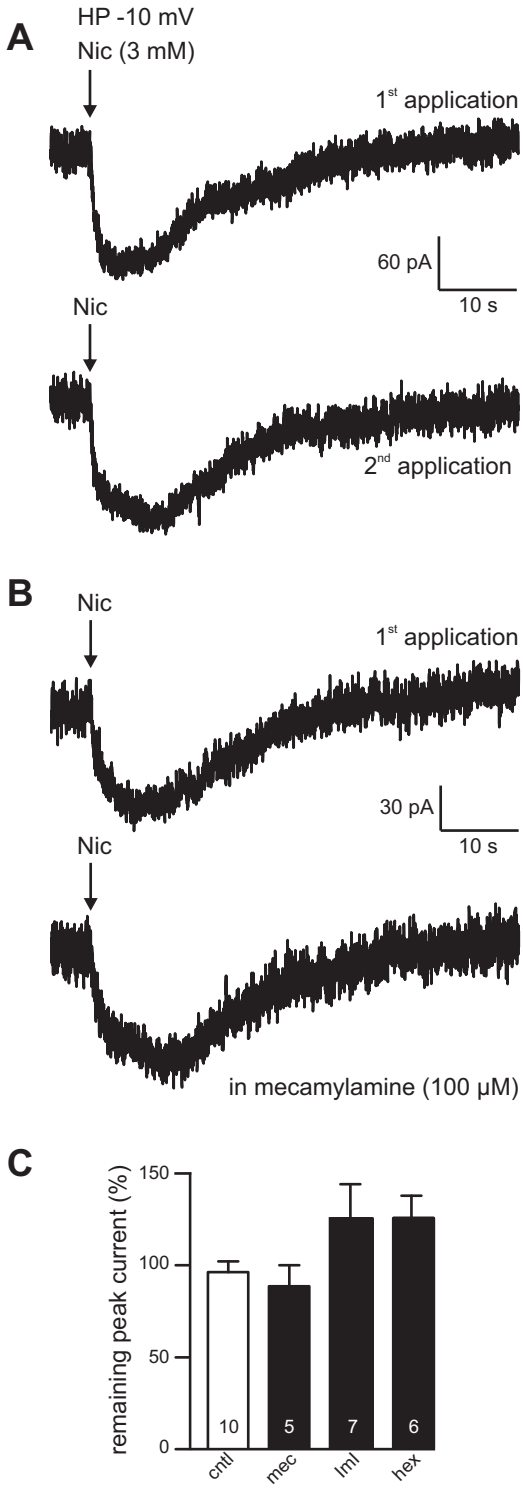

Fig. 4. Antagonist profile for the nicotine-evoked response at −10 mV. Shown are responses to 10 s of pressured-applied 3 mM nicotine (Nic) in cultured bag cell neurons under whole cell voltage-clamp at a −10 mV holding potential (HP) in nASW with K^+-based internal solution. *A*, *top*: in control, the response evoked by the first nicotine application was very similar to that produced 10 min later by the second application (*bottom*). Because there was no desensitization, antagonists were evaluated by delivering drug during the intervening period and measuring any change between the initial and latter response. Scale bars apply to both traces. *B*: in a separate neuron, bath delivery of 100 μM mecamylamine, a nicotinic receptor blocker, did not alter the second response evoked by pressure-applied nicotine. Scale bars apply to both traces. *C*: summary data showing the percentage of remaining current between the second and first nicotine applications. None of the classical nicotinic receptor blockers, i.e., mecamylamine (mec), α-conotoxin ImI (ImI), or hexamethonium (hex), significantly altered the magnitude of the nicotine-evoked response (ordinary ANOVA). Numbers in bars indicate number of neurons.

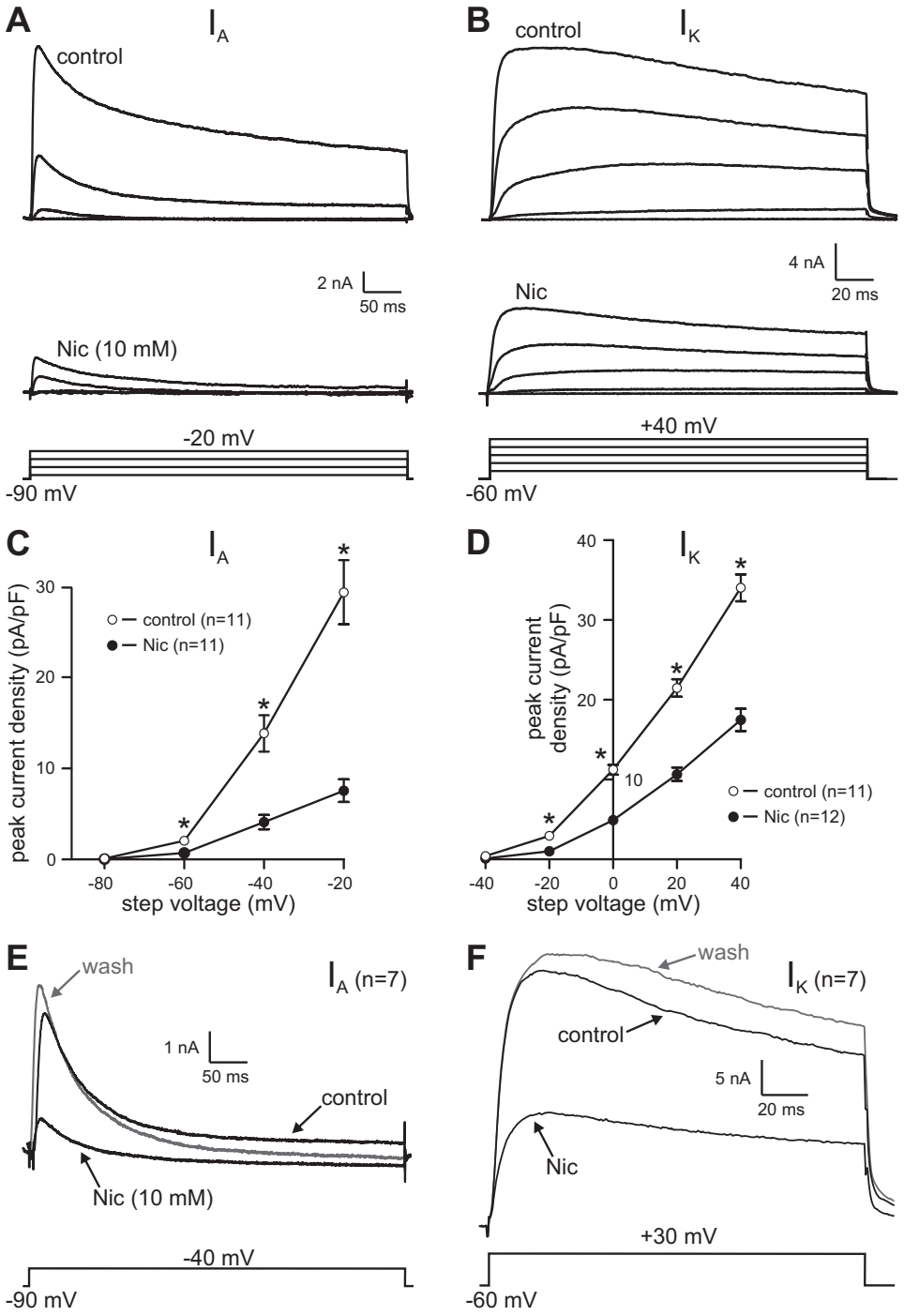

Fig. 5. Nicotine reversibly reduces both the A-type (I_A) and delayed-rectifier (I_K) K^+ current. K^+ currents were recorded from cultured bag cell neurons under whole cell voltage-clamp using K^+-based intracellular solution and ASW where Na^+ and Ca^{2+} were replaced with $NMDG^+$ and Mg^{2+}, respectively. *A*: from a holding potential of −90 mV, 500-ms steps to −80, −60, −40, and −20 mV (*bottom*) elicited inactivating I_A (*top*). After a 10-min perfusion of 10 mM nicotine (Nic), I_A was reduced at all test voltages (*middle*). Scale bars apply to both sets of traces. *B*: chiefly noninactivating I_K (*top*) were evoked from a holding potential of −60 mV by 200-ms steps to −40, −20, 0, +20, and +40 mV (*bottom*). I_K was also diminished by about half with nicotine, beginning at the −20-mV pulse (*middle*). Scale bars apply to both sets of traces. *C*: nicotine significantly decreased I_A at −60 and −40 mV (both $^*P < 0.05$, Mann-Whitney *U*-test), as well as at −20 mV ($^*P < 0.001$, unpaired Student's *t*-test, Welch corrected). *D*: similarly, nicotine led to a significant drop in I_K at −20 mV ($^*P < 0.01$, unpaired Student's *t*-test, Welch corrected), at 0 and +20 mV (both $^*P < 0.001$, Mann-Whitney *U*-test), and at +40 mV ($^*P < 0.001$, unpaired Student's *t*-test). *E*: from a holding potential of −90 mV, a single 500-ms step to −40 mV (*bottom*) triggered an I_A (*top*) from a cultured bag cell neuron under whole cell voltage-clamp. After a 10-min wait period, 10 mM nicotine was microperfused for 30 s, during which a second pulse to −90 mV resulted in a peak current that was ~25% of control. Moreover, after 10 min of wash with nASW, a third step produced a current similar to control (gray trace). Data are representative of $n = 7$ neurons. *F*: in the same neuron, an I_K current (*top*) was elicited by a 200-ms pulse from −60 to +30 mV (*bottom*). Again, subsequent to a 10-min interval, perfusion of nicotine decreased the current by about two-thirds, which was reversed upon wash to nASW for 10 min (gray trace).

ing, fast-inactivating current, which was reduced after nicotine and fully recovered following 10 min of wash (Fig. 5*E*, *top*). Nicotine led to a significant decrease in the average peak I_A density by ~75%, which returned to control levels upon wash (4.20 ± 0.63 pA/pF in control vs. 1.00 ± 0.23 pA/pF in nicotine vs. 4.53 ± 0.66 pA/pF in wash; $n = 7$; $P < 0.0001$, repeated-measures ANOVA; $P < 0.05$, Dunnett multiple comparisons posttest). For I_K, a characteristic slowly inactivating current was induced with the 200-ms step to +30 mV (Fig. 5*F*, *bottom*). In a manner similar to that for I_A, nicotine perfusion clearly reduced I_K, which completely recovered during wash for 10 min (Fig. 5*F*, *top*). The mean peak I_K density was significantly lowered by around two-thirds, but this was completely restored upon return to normal extracellular saline (31.56 ± 3.69 pA/pF in control vs. 11.76 ± 1.17 pA/pF in nicotine vs. 33.50 ± 4.21 pA/pF in wash; $n = 7$; $P < 0.0001$, repeated-measures ANOVA; $P < 0.05$, Dunnett multiple comparisons posttest).

Strong and Kaczmarek (1986) demonstrated that I_K can be separated into two components, one fast and the other slow, by fitting the tail currents elicited upon return to negative potentials from strong depolarization. Moreover, based on the considerable variation in the ratio of the slow to the fast component, as well as the two components being differentially mod-

ulated by cAMP, they concluded that the components represented two distinct voltage-dependent delayed-rectifier K^+ currents. Using a protocol similar to theirs, we held neurons at −50 mV and delivered five 100-ms steps to +30 mV at 0.2 Hz, with the interstep interval incorporating a P/4 leak subtraction protocol (Fig. 6*A*, *bottom*). The resulting currents were averaged, and the tail current following repolarization to −50 mV was fit with a two-term exponential decay (τ_{fast} representing the inactivating component and τ_{slow} representing the sustained component of I_K, respectively). A typical control current ($n = 12$) is displayed in Fig. 6*A*, *top*, with the approximate locations of the two time constants. The average τ_{fast} was ~1 ms, whereas τ_{slow} was ~11 ms (Fig. 6*B*). As expected, the peak current was lowered by about twofold when 10 mM nicotine ($n = 13$) was delivered to the bath (31.3 ± 1.2 pA/pF in control vs. 14.9 ± 1.1 pA/pF in nicotine; $P < 0.0001$, unpaired Student's *t*-test; Fig. 6*A*, *middle)*. However, nicotine inhibited both components of I_K, because neither τ_{fast} nor τ_{slow} were changed and the summary data showed the time constants to be not significantly different from control (Fig. 6*B*).

Inhibition of K^+ channels by nicotine is rapid. If nicotine is acting as blocker, there is some expectation that the K^+ channel inhibition would be rapid (Cooper et al. 2003). Consistent with this, the onset of the nicotine-evoked response at −10 mV appeared to be at least 1 s during certain pressure-application experiments (e.g., see Fig. 3*C* or Fig. 4, *A* and *B*). To more accurately test the kinetics of the nicotine-mediated block, we pressure-applied agonist during a step protocol designed to repeatedly activate I_K. The initial experiment involved delivering a 20-s, 8-Hz train of 100-ms voltage steps from −50 to +30 mV while pressure-applying either 10 mM nicotine or 100 μM epibatidine for 10 s, starting at the 4-s mark. Because of the pulse frequency during the stimulus train, currents were not leak subtracted (Fig. 7*A*, *inset*). Epibatidine, an alkaloid from the frog, *Epipdobates*, was selected as a control for any pressure artifacts both because of its structural similarity to nicotine (Badio and Daly 1994) and because epibatidine failed to activate a current in bag cell neurons at resting (−60 mV) or depolarized potentials (−10 mV; $n = 3$; data not shown). Epibatidine was dissolved in nASW at as high a concentration as we found possible. I_K underwent use-dependent inactivation, judging by an immediate reduction in peak current, which fell quickly over the first 2 s but then slowed to a gradual and continuous decline for the remainder of the train (Fig. 7*A*). During pressure application of epibatidine ($n = 7$), aside from the ongoing use-dependent inactivation, there was no apparent change in the magnitude of the peak current (Fig. 7*A*, filled circles, *left inset*). In contrast, when nicotine was introduced ($n = 8$), the I_K dropped suddenly but then returned to preblock levels almost as quickly when the nicotine application had ceased (Fig. 7*A*, open circles, *right inset*). This reduction took place within 250 ms of pressure-application onset and reached a maximum by ~3 s of nicotine delivery (Fig. 7*B*, *right*); such changes were not evident during epibatidine application (Fig. 7*B*, *left*). The average maximal decrease in peak current due to nicotine was significantly larger, at ~550 pA, compared with that in epibatidine, at ~15 pA (Fig. 7*C*).

Subsequently, experiments were undertaken to more closely examine the possibility that nicotine was hastening the use-dependent inactivation of I_K. Specifically, we added nicotine alone and then later compared the extent of block with and without continuous stimulation up to that point. All neurons were first given a single, 100-ms step from −50 to +30 mV to elicit I_K, and then 5 min later, 10 mM nicotine was pressure-applied for 10 s. For nonstimulated cells, a second, solitary step to +30 mV was delivered 8 s after the onset of nicotine, whereas for stimulated cells, use-dependent inactivation was brought about by an 8-Hz, 5-s train of steps to +30 mV that was started 3 s after nicotine was introduced. The final step of the train stimulus was delivered at the same time as when the single step was given to nonstimulated neurons (Fig. 7*D*, *top*). The step prior to nicotine was given to all neurons to provide both a means to normalize some of the ensuing data and to be more certain that any differences were not due to cell-to-cell variability in current density. The degree of K^+ current inhibition in nicotine was greater with ongoing use-dependent inactivation from the stimulation (Fig. 7*D*, *bottom right*) than without stimulation (Fig. 7*D*, *bottom left*). In particular, compared with the peak current from the step prior to nicotine, there was a significantly greater decrease by the final step of the train stimulus in nicotine (stimulated; $n = 5$) than by the solitary step in nicotine (nonstimulated; $n = 5$; Fig. 7*E*, *top*). Moreover, the density of the current evoked by the final step of the train stimulus in nicotine was significantly smaller than that of the solitary step in nicotine (Fig. 7*E*, *bottom*).

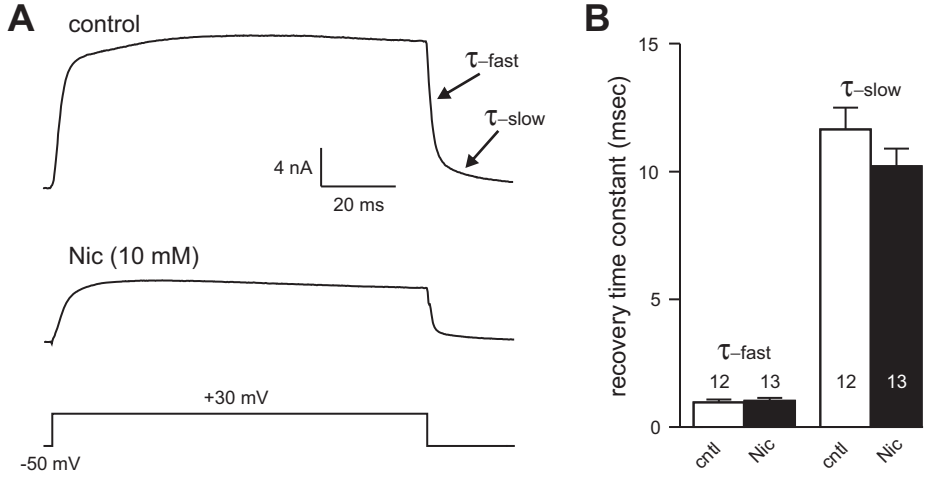

Fig. 6. Nicotine inhibits both components of the delayed-rectifier K^+ current. *A*: in a whole cell voltage-clamped cultured bag cell neuron, the biexponential tail current of I_K is apparent following a 100-ms step to +30 mV from a holding potential of −50 mV (*bottom*). A two-term exponential fit of the tail current yields fast (τ_{fast}) and slow (τ_{slow}) time constants. In control (top), the current reflects an average of 5 steps, with the approximate placement of τ_{fast} and τ_{slow} as indicated. After 10 min of 10 mM nicotine (Nic), the magnitude of I_K was smaller (*middle*), although the tail current was similar to control. Scale bars apply to both traces. *B*: despite a reduced I_K magnitude with nicotine, the summary data reveal no significant difference between control and nicotine for either τ_{fast} or τ_{slow} (both unpaired Student's *t*-test). Numbers in bars indicate number of neurons.

Finally, we also compared two groups of neurons where either 10 mM nicotine or simply nASW was pressure-applied for 10 s and the 8-Hz, 5-s train of steps to +30 mV was given 3 s into the pressure application. The peak current evoked by the first pulse was divided into itself as well as all of the subsequent currents elicited by the train stimulus for a given neuron. These data were then averaged and fit with a two-term exponential function. Whereas the slow time constant from the fits was similar between the two groups (data not shown), the fast time constant showed a difference. Specifically, the use-dependent inactivation in nicotine was significantly quicker than in nASW ($\tau_{\text{fast-nicotine}} = 98.42 \pm 10.98$ ms, $n = 5$, vs. $\tau_{\text{fast-nASW}} = 223.7 \pm 64.15$ ms, $n = 8$; $P < 0.02$, Mann-Whitney *U*-test).

Short-term nicotine pretreatment increases excitability. The effects of nicotine on steady-state current at depolarized potentials, as well as on voltage-gated I_A and I_K, is likely to have physiological consequences. Therefore, we tested whether pretreating cultured bag cell neurons for 10 min with 10 mM nicotine altered action potential dynamics or changed the ability to fire action potentials to a prolonged stimulus. Membrane potential recordings were made from neurons, and bias current was used to set them at −60 mV (see MATERIALS AND METHODS, *Sharp-electrode current-clamp recording*). For the pretreated cells, nicotine caused a 15.1 ± 6.9-mV depolarization ($n = 9$; data not shown) that recovered completely to −60 mV by the end of the 10 min. Our prior work, involving pressure application or brief periods of perfusion, showed that nicotine resulted in a change in membrane potential from −60 mV that was transient due to desensitization (White et al. 2014). Thus, in the present study, by the end of the 10-min nicotine pretreatment, any ionotropic receptors were closed and desensitized, and the only effect remaining was that of nicotine blocking mainly voltage-gated K^+ currents.

A 1-nA, 50-ms stimulus (Fig. 8*A*, *bottom*) was delivered to elicit a single action potential from −60 mV. In control neurons ($n = 9$), the action potential took ~27 ms to reach a peak amplitude of ~75 mV with a half-width of ~8 ms (Fig. 8*A*, *middle*). However, in parallel neurons treated with nicotine ($n = 9$), the action potential reached peak in a faster time of ~20 ms, with a larger magnitude of ~90 mV and a broader half-width of ~17 ms (Fig. 8*A*, *top*). On average, all three action potential parameters were significantly different in nicotine (Fig. 8*C–E*). Also, the current required to evoke a single action potential was reduced by nicotine (0.78 ± 0.08 nA in control vs. 0.38 ± 0.04 nA in nicotine; $P < 0.01$, Mann-Whitney *U*-test) without significantly affecting the input resistance, as determined from a resting potential of −60 mV by a −50-pA current pulse (308 ± 46 MΩ in control vs. 378 ± 38 MΩ for nicotine; $P > 0.05$, Mann-Whitney *U*-test).

To investigate possible changes to excitability brought about by nicotine, neurons were subjected to a 10-s depolarizing current pulse of between 200 and 800 pA, which corresponded to the observed rheobase for each given cell (Fig. 8*B*, *bottom*). Under control conditions, the 10-s current generated an initial burst that averaged fewer than 10 action potentials, followed by silence for the remainder of the stimulus (Fig. 8*B*, *middle*, and *E*). Conversely, the excitability of neurons that saw nicotine was increased, based on continuous firing during the 10-s current (Fig. 8*B*, *top*). The output following nicotine treatment was a significantly larger action potential production, with a mean of over 50 spikes (Fig. 8*E*).

DISCUSSION

Nicotine is generally considered an agonist that opens ionotropic cholinergic receptors (Albuquerque et al. 2009; Gardner et al. 1984; Langley 1905). Using *Aplysia* bag cell neurons, we have now shown that nicotine can cause apparent inward current by reducing one or more K^+ currents. Consistent with K^+ channel closure, this response is accompanied by a decline in membrane conductance, is prominent at depolarized potentials, is prevented by intracellular perfusion with Cs^+-based intracellular saline, and results in the appearance of negative slope in the *I/V* relationship. Exposure of bag cell neurons to nicotine also leads to changes in excitability that are in keeping with a lessening of I_A and I_K. A decrease in voltage-gated K^+ channels, by either regulation or direct block, can have profound effects on neuronal properties (Byrne and Kandel 1996; Levitan and Kaczmarek 2002); accordingly, we observed faster spike onset and larger/broader action potentials, as well as a greater number of spikes, in response to stimulation.

Although the evidence mainly points to nicotine acting as a K^+ channel blocker, a genuine nicotinic receptor could be involved. If such a receptor exists, it does not appear to use classical metabotropic signaling, given the inability of the G protein blocker GDPβS to alter the nicotine-evoked current at −10 mV. Furthermore, it is unlikely that the nicotine response described in this report is due to activation of either of the previously characterized bag cell neuron cholinergic receptors, i.e., the distinct inward currents induced by acetylcholine or nicotine at −60 mV (White and Magoski 2012; White et al. 2014). Both of those responses are associated with an increase in membrane conductance, are unaffected by intracellular Cs^+ perfusion, are inwardly rectifying with depolarization, and do not pass current at −10 mV. Whereas the present study finds that none of the established nicotinic receptor antagonists impact the nicotine-evoked response at −10 mV, our prior work showed that mecamylamine antagonizes both the acetylcholine- and nicotine-elicited currents at −60 mV, whereas α-conotoxin ImI and hexamethonium exclusively inhibit the acetylcholine response (White and Magoski 2012; White et al. 2014). Finally, the nicotine-evoked response at −10 mV has a Hill slope of ~1 and an EC_{50} of ~1.5 mM; this is dissimilar from the current elicited by nicotine at −60 mV, which presents a Hill slope of ~ 2.5 and an EC_{50} of ~250 μM (White et al. 2014).

Cockroach dorsal unpaired median neurons also respond to nicotine with a decrease-conductance current (Courjaret and Lapied 2001; Thany et al. 2008). Like that in *Aplysia*, this current is K^+ permeable and sensitive to intracellular Cs^+ perfusion; however, unlike the *Aplysia* current, the *Periplanta* current is inhibited by mecamylamine and α-conotoxin ImI. Those authors did not directly test nicotine on K^+ currents; rather, they concluded that nicotine binding closed a constitutively active atypical nicotinic receptor. In rat striatal neurons, nicotine and the nicotinic agonist dimethylphenyl pyperazinium inhibit I_K but not I_A (Hamon et al. 1997). Although this effect is not sensitive to mecamylamine, hexamethonium, D-tubocurarine, or the G_i/G_o protein inhibitor pertussis toxin, a nicotine receptor is still implicated based on a block by the

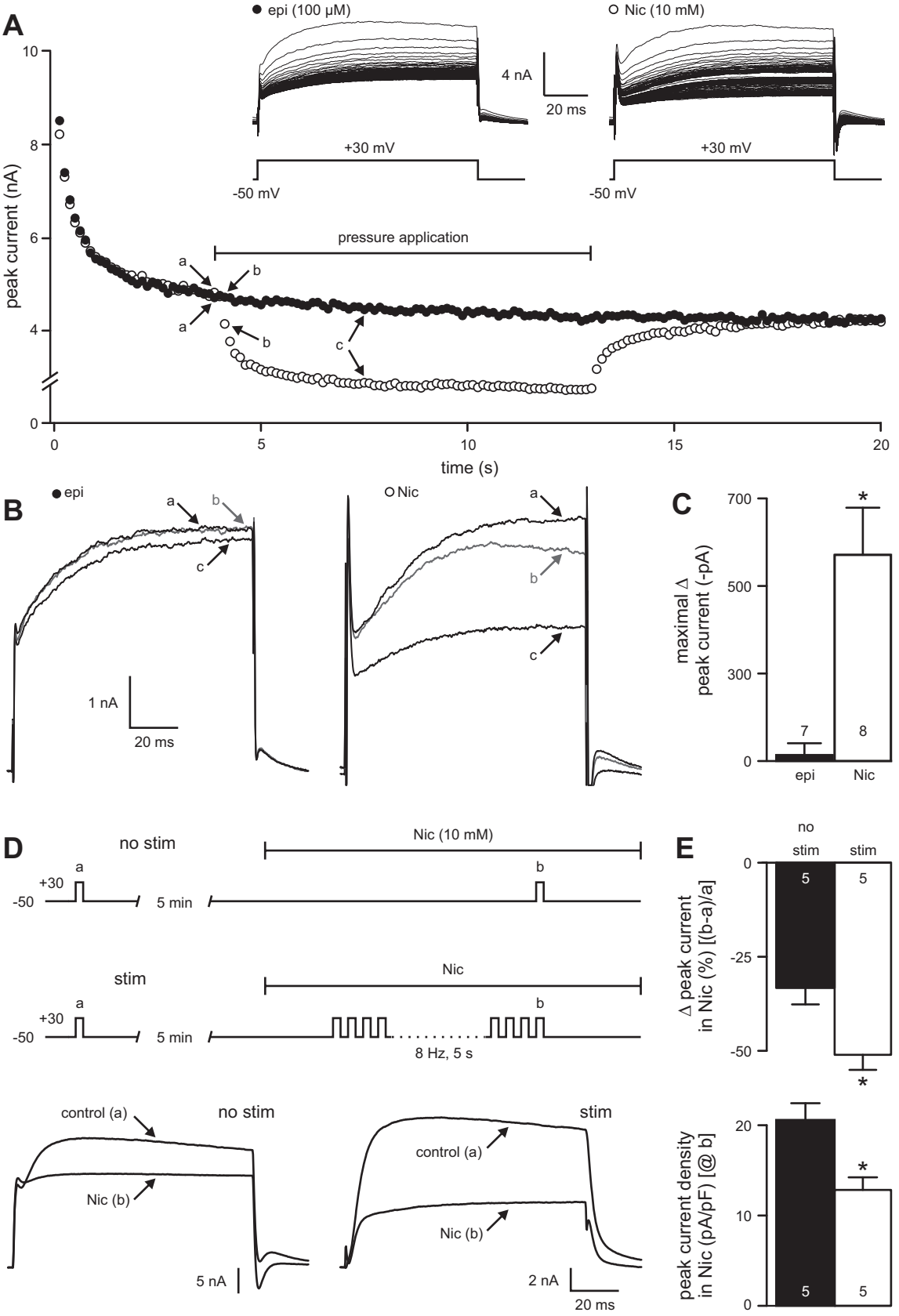
A
epi (100 μM)
Nic (10 mM)
4 nA
20 ms
+30 mV
-50 mV
+30 mV
-50 mV
pressure application
peak current (nA)
time (s)
a
b
c
B
epi
Nic
1 nA
20 ms
C
maximal Δ peak current (-pA)
epi
Nic
D
no stim
Nic (10 mM)
+30
-50
5 min
stim
Nic
8 Hz, 5 s
control (a)
Nic (b)
5 nA
2 nA
20 ms
E
no stim
stim
Δ peak current in Nic (%) [(b-a)/a]
peak current density in Nic (pA/pF) [@ b]

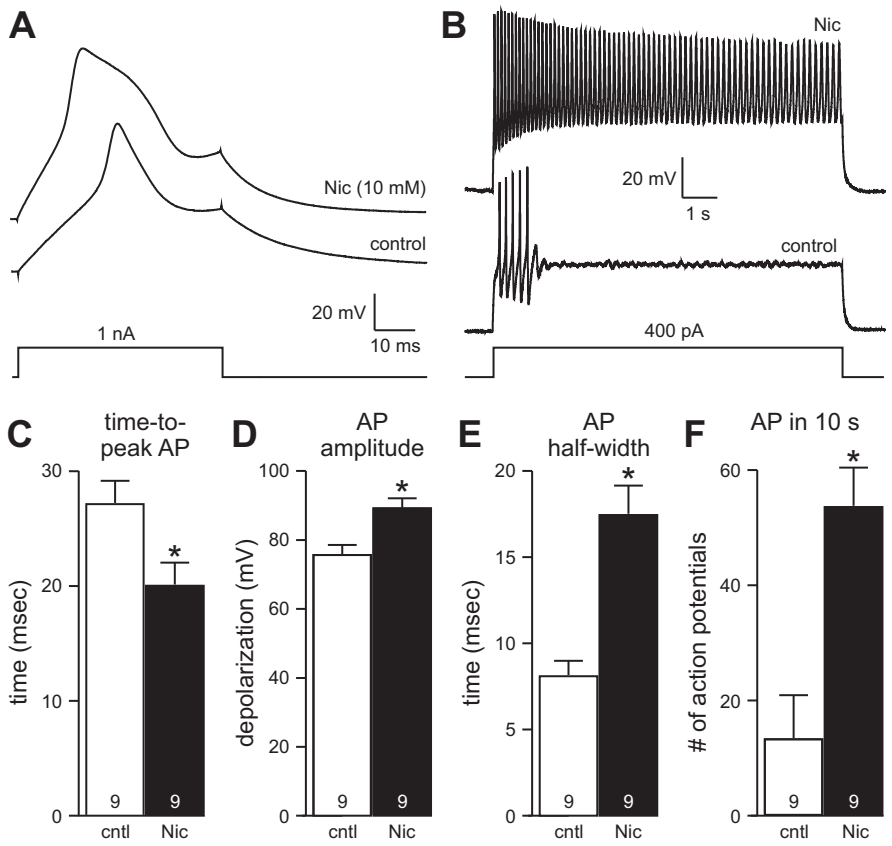

Fig. 8. Nicotine pretreatment increases the excitability of bag cell neurons. In nASW, cultured bag cell neurons were initially set to −60 mV with constant bias current under sharp-electrode current clamp. *A*: a 50-ms, 1-nA depolarizing pulse (*bottom*) generated a single action potential in a control cell that peaked by ~30 ms (*middle*). When a different neuron was pretreated for ~10 min in 10 mM nicotine (Nic), the action potential occurred sooner, had a larger amplitude, and was broader (*top*). Scale bars apply to both traces. *B*: in the same control neuron as in *A*, a 10-s, 400-pA current step (*bottom*) only elicited 5 action potentials before accommodating (*middle*). However, the nicotine-treated neuron fired continuously and at a higher frequency (*top*) throughout the stimulus. Scale bars apply to both traces. *C–E*: summary data indicate nicotine pretreatment significantly reduced the time to peak action potential (AP) (*C*; $*P < 0.05$, unpaired Student's *t*-test), increased the amplitude (*D*; $*P < 0.05$, unpaired Student's *t*-test), and broadened the half-width (*E*; $*P < 0.001$, unpaired Mann-Whitney *U*-test). Numbers in bars indicate number of neurons. *F*: the excitability of bag cell neurons was enhanced, based on a significant 3-fold increase in the number of action potentials brought about by a 10-s current pulse matching the individual rheobase of the cells in question ($*P < 0.001$, unpaired Mann-Whitney *U*-test). Numbers in bars indicate number of neurons.

competitive antagonist dihydro-β-erythroidine. These findings are disparate from those in bag cell neurons, where nicotine reduces multiple K^+ currents: steady state at −10 mV as well as I_A and I_K.

Although nicotinic receptors typically function solely as ion channels, there are a few cases of coupling to second messengers. For mouse myotubes, nicotine mediates an increase in intracellular Ca^{2+} that necessitates both Na^+ influx through the nicotinic receptor and inositol triphosphate production but is not affected by nicotinic antagonists or pertussis toxin (Grassi et al. 1993). Activation of α7-nicotinic receptors in rat microglia also elevates Ca^{2+}, but it is not associated with any form of ionic current (Suzuki et al. 2006). Similarly, in specific *Aplysia* neurons, binding of nicotine to Cl^--permeable nicotinic receptors turns on lipoxygenase and can be prevented by pertussis toxin but does not require Cl^- influx per se. (Tieman et al. 2001). Such examples aside, these transduction pathways probably do not play a role in the nicotine-mediated effects described in the present study. GDPβS does not modify the nicotine-evoked response at −10 mV, and the rapid nature by which nicotine inhibits I_K (within 250 ms) seems too brief for second messenger-based signaling. Our laboratory and others have found that currents or membrane potential changes brought about by metabotropic receptors in *Aplysia* neurons

Fig. 7. Inhibition of K^+ current by nicotine has a rapid time course. *A*: I_K was evoked from cultured bag cell neurons under whole cell voltage-clamp with 100-ms steps from −50 to +30 mV delivered at 8 Hz for 20 s. *Insets*: overlays of currents induced by the train when either 100 μM epibatidine (epi; *left*) or 10 mM nicotine (Nic; *right*) were introduced about one-third into the duration of the stimulation. Scale bars apply to both sets of traces. Graph shows peak current vs. time for the 2 cells; use-dependent inactivation was rather abrupt at the outset but slowed to a more gradual decline by ~2 s. Approximately 4 s into the train, a 10-s pressure application of agonist began (at horizontal bar). In conjunction with nicotine (open circles), the peak outward current was reduced within ~250 ms. To control for pressure artifacts, 100 μM of the structurally similar amine epibatidine (filled circles) was pressure ejected onto a second neuron, but the peak current maintained a stable decay. Arrows indicating *a*, *b*, and *c* correspond to sweeps displayed in *B*. *B*: current traces immediately before (*a*), 250 ms after (*b*; gray trace), and 3.625 s after (*c*) the onset of epibatidine (*left*) or nicotine (*right*) pressure ejection. In the case of nicotine, there was a clear drop at both time points subsequent to delivery; for epibatidine, the only change was the small decrease associated with the ongoing use-dependent inactivation. Scale bars apply to both sets of traces. *C*: summary data indicating the average maximal reduction in peak current as a result of nicotine is significantly larger than that resulting from epibatidine ($*P < 0.01$, unpaired Student's *t*-test, Welch corrected). *D*, *top*: outline of protocol used to further examine the impact of nicotine on I_K use-dependent inactivation. Initially, current is induced in all neurons (from 2 separate groups) with a single 100-ms step from −50 to +30 mV (*time point a*). Five min later, 10 mM nicotine is pressure-applied for 10 s. Cells in the nonstimulated group (no stim) receive another single step to +30 mV at 8 s following the start of nicotine. For neurons in the stimulated group (stim), use-dependent inactivation is set off with an 8-Hz, 5-s train of steps to +30 mV that begins 3 s after nicotine. The last step of the train-stimulus occurs at the same time as the single step given to nonstimulated neurons (*time point b*). *Bottom*, current traces in control conditions before nicotine (*a*) and from either the solitary step in a nonstimulated neuron or the final pulse of the train-stimulus in a stimulated neuron (both *b*). The extent of inhibition by nicotine is more pronounced during use-dependent inactivation, i.e., with stimulation than without stimulation. Time base applies to both sets of traces. *E*, *top*: group data of the percent change in peak current [(*time point b* − *time point a*)/*time point a*] comparing the step before nicotine with either the single step in nicotine (no stim) or the last step of the train stimulus in nicotine (stim). Stimulation results in significantly more inhibition by nicotine ($*P < 0.02$, unpaired Student's *t*-test). *Bottom*, the last step of the train stimulus in nicotine elicits current with a peak density that is significantly less than that from the single step in nicotine (both taken at *time point b*) ($*P < 0.02$, unpaired Student's *t*-test). Numbers in bars indicate number of neurons.

operate on a timescale of seconds to minutes, as opposed to milliseconds (Bolshakov et al. 1993; Fisher et al. 1993; Tam et al. 2011; White and Magoski 2012). Parenthetically, we reported earlier that nicotine fails to alter bag cell neuron intracellular Ca^{2+} under voltage clamp (White et al. 2014).

Rather than a nicotinic receptor, the pharmacological data largely indicate block of K^+ channels as the mechanism underlying both the nicotine-evoked response at −10 mV and the reduction of I_A and I_K by nicotine in bag cell neurons. In addition, both time constants that describe the I_K tail current are unaltered by nicotine, suggesting that the two delayed rectifiers comprising I_K were equally blocked. A-type and inward-rectifier K^+ currents are inhibited by nicotine in canine ventricular myocytes or when the corresponding genes (K_V4.3, K_{IR}2.1, K_{IR}2.2) are expressed in oocytes (Wang et al. 2000a, 2000b). Although those studies do not denote a time course for the action of nicotine, they do report that nicotine enhances use-dependent inactivation and that the block is not prevented by mecamylamine. K^+ channels in rat tail artery smooth muscle cells are also sensitive to nicotine, i.e., millimolar levels block delayed-rectifier currents in a near-instantaneous and fully reversible manner (Tang et al. 1999). Unsurprisingly, the effect of nicotine on smooth muscle is not altered by dihydro-β-erythroidine.

The inhibition of bag cell neuron I_A and I_K following bath application or perfusion of nicotine, with no intervening test pulses, suggests the drug may bind to K^+ channels that are closed. That stated, we also observe a seeming acceleration of I_K use-dependent inactivation by nicotine. Specifically, giving nicotine prior to repetitive stimulation of I_K results in a greater rundown of the current compared with unstimulated neurons that are exposed to nicotine or cells that receive control applications of nASW. Similar tonic and use-dependent blocks are reported by Wang et al. (2000a) for ventricular myocytes. With respect to the nicotine-evoked response at −10 mV, this represents the closure of steady-state K^+ channels that are open when bag cell neurons are held at −10 mV. At this voltage, I_A will fully inactivate in a short period of time, but a small proportion of I_K is still available (Strong 1984; Strong and Kaczmarek 1986). Hence, nicotine may affect some fraction of I_K that has not inactivated and/or a leak K^+ channel. However, in keeping with a more specific action on voltage-dependent K^+ currents, the negative-slope current appears only as the membrane potential approaches −30 mV. Moreover, nicotine does not change input resistance measured from −60 mV, where it is likely that I_A is completely closed and there is only modest activation of I_K, leaving few channels for nicotine to block. Nicotine may be acting like TEA, a classical blocker (Hille 2001; Lorente de Nó 1949) which also inhibits voltage-gated K^+ channels at millimolar concentrations in neurons from *Aplysia*, including bag cell neurons (Hermann and Gorman 1981; Quattrocki et al. 1994; Strong and Kaczmarek 1986), as well the pulmonate molluscs, *Helix* and *Onchidiuma* (Hagiwara and Saito 1959; Neher and Lux 1972). Potentially, the *N*-methyl group of the pyrrole ring on nicotine may be occluding the outer pore region of the channels in a fashion similar to the *N*-ethyl groups of TEA (MacKinnon and Yellen 1990).

During the afterdischarge, a reduction of K^+ currents by phosphorylation enhances bag cell neuron excitability (Kaczmarek et al. 1980; Kaczmarek and Strumwasser 1984; Strong 1984; Strong and Kaczmarek 1986; Zhang et al. 2004), and this is mimicked by exogenous nicotine. The negative-slope *I/V* that results from nicotine block of K^+ channels markedly elevates the spiking response to prolonged current injection (Beilby 1986; Lüthi et al. 1997; Shen and Johnson 2013; Wilson and Wachtel 1974). Also, the speeding up of action potential generation in nicotine is ostensibly due to the reduction in I_A, which normally serves to limit action potential initiation by activating near resting potential (Connor and Stevens 1971; Gustafsson et al. 1982; Strong 1984). Finally, the drop in I_K induced by nicotine likely enhances spike height and width, consistent with a role for delayed-rectifier K^+ currents in controlling action potential dynamics at more depolarized voltages (Connor and Stevens 1971; Hagiwara and Saito 1959; Klein and Kandel 1978; Quattrocki et al. 1994; Strong and Kaczmarek 1986).

The consequences of nicotine exposure in bag cell neurons may be applicable to the noncanonical effects of nicotine in both the heart and brain of other organisms, particularly in cases of nicotine poisoning, which often involve higher doses compared with that from smoking (Mayer 2014). For *Aplysia*, the shoreline marine environment has the potential to be contaminated with nicotine/neonicotinoids from pesticide runoff (Dondero et al. 2010; Felsot et al. 2002). In turn, this could alter reproductive outcomes in the mollusc by chronically blocking bag cell neuron K^+ channels.

ACKNOWLEDGMENTS

We thank H. M. Hodgson for technical assistance, G. Z. Zhu for aiding in some data analysis, C. J. Groten and N. M. Magoski for critical evaluation of previous drafts of the manuscript, and the anonymous reviewers for constructive criticism of the work.

GRANTS

This work was supported by a Canadian Institutes of Health Research (CIHR) operating grant (to N. S. Magoski). S. H. White held a McLaughlin/Bracken Scholarship and a Queen Elizabeth II in Science Technology Scholarship. N. S. Magoski held a CIHR New Investigator Award.

DISCLOSURES

No conflicts of interest, financial or otherwise, are declared by the authors.

AUTHOR CONTRIBUTIONS

S.H.W., R.M.S., and N.S.M. conception and design of research; S.H.W. and R.M.S. performed experiments; S.H.W., R.M.S., and N.S.M. analyzed data; S.H.W., R.M.S., and N.S.M. interpreted results of experiments; S.H.W., R.M.S., and N.S.M. prepared figures; S.H.W. drafted manuscript; S.H.W., R.M.S., and N.S.M. edited and revised manuscript; R.M.S. and N.S.M. approved final version of manuscript.

REFERENCES

Adelman WJ Jr, Senft JP. Voltage clamp studies on the effect of internal cesium ion on sodium and potassium currents in the squid giant axon. *J Gen Physiol* 50: 279–293, 1966.

Albuquerque EX, Pereira EF, Alkondon M, Rogers SW. Mammalian nicotinic acetylcholine receptors: from structure to function. *Physiol Rev* 89: 73–120, 2009.

Arch S. Polypeptide secretion from the isolated parietovisceral ganglion of *Aplysia californica*. *J Gen Physiol* 59: 47–59, 1972.

Ascher P, Large WA, Rang HP. Two modes of action of ganglionic blocking-drugs. *Br J Pharmacol* 66: 79P, 1979.

Ascher P, Marty A, Neild TO. Mode of action of antagonists of excitatory response to acetylcholine in *Aplysia* neurons. *J Physiol* 278: 207–235, 1978.

Badio B, Daly JW. Epibatidine, a potent analgetic and nicotinic agonist. *Mol Pharmacol* 45: 563–569, 1994.

Beilby MJ. Factors controlling the K^+ conductance in *Chara*. *J Membr Biol* 93: 187–193, 1986.

Bezanilla F, Armstrong CM. Inactivation of the sodium channel. I. Sodium current experiments. *J Gen Physiol* 70: 549–566, 1977.

Bolshakov VY, Gapon SA, Katchman AN, Magazanik LG. Activation of a common potassium channel in molluscan neurones by glutamate, dopamine and muscarinic agonist. *J Physiol* 468: 11–33, 1993.

Brezina V, Eckert R, Erxleben C. Suppression of calcium current by an endogenous neuropeptide in neurones of *Aplysia californica*. *J Physiol* 388: 565–595, 1987.

Brown DA, Adams PR. Muscarinic suppression of a novel voltage-sensitive K^+-current in a vertebrate neurone. *Nature* 283: 673–676, 1980.

Byrne JH, Kandel ER. Presynaptic facilitation revisited: state and time dependence. *J Neurosci* 16: 425–435, 1996.

Carew TJ, Kandel ER. Inking in *Aplysia californica*. III. Two different synaptic conductance mechanisms for triggering central program for inking. *J Neurophysiol* 40: 721–734, 1977.

Carlin KP, Jones KE, Jiang Z, Jordan LM, Brownstone RM. Dendritic L-type calcium currents in mouse spinal motoneurons: implications for bistability. *Eur J Neurosci* 12: 1635–1646, 2000.

Coggeshall RE. A light and electron microscope study of the abdominal ganglion of *Aplysia californica*. *J Neurophysiol* 30: 1263–1287, 1967.

Conn PJ, Kaczmarek LK. The bag cell neurons of *Aplysia*. *Mol Neurobiol* 3: 237–273, 1989.

Connor JA, Stevens CF. Prediction of repetitive firing behaviour from voltage clamp data on an isolated neurone soma. *J Physiol* 213: 31–53, 1971.

Cooper JR, Bloom FE, Roth RH. *The Biochemical Basis of Neuropharmacology*. New York, NY: Oxford University Press, 2003.

Courjaret R, Lapied B. Complex intracellular messenger pathways regulate one type of neuronal alpha-bungarotoxin-resistant nicotinic acetylcholine receptors expressed in insect neurosecretory cells (dorsal unpaired median neurons). *Mol Pharmacol* 60: 80–91, 2001.

Dargaei Z, Colmers PL, Hodgson HM, Magoski NS. Electrical coupling between *Aplysia* bag cell neurons: characterization and role in synchronous firing. *J Neurophysiol* 112: 2680–2696, 2014.

Dondero F, Negri A, Boatti L, Marsano F, Mignone F, Viarengo A. Transcriptomic and proteomic effects of a neonicotinoid insecticide mixture in the marine mussel (*Mytilus galloprovincialis*, Lam.). *Sci Total Environ* 408: 3775–3786, 2010.

Eckert R, Lux HD. A voltage-sensitive persistent calcium conductance in neuronal somata of *Helix*. *J Physiol* 254: 129–151, 1976.

Eckstein F, Cassel D, Levkovitz H, Lowe M, Selinger Z. Guanosine 5′-*O*-(2-thiodiphosphate). An inhibitor of adenylate-cyclase stimulation by guanine-nucleotides and fluoride ions. *J Biol Chem* 254: 9829–9834, 1979.

Ellison M, McIntosh JM, Olivera BM. Alpha-conotoxins ImI and ImII. Similar alpha 7 nicotinic receptor antagonists act at different sites. *J Biol Chem* 278: 757–764, 2003.

Felsot AS, Ruppert JR. Imidacloprid residues in Willapa Bay (Washington State) water and sediment following application for control of burrowing shrimp. *J Agric Food Chem* 50: 4417–4423, 2002.

Ferguson GP, ter Maat A, Pinsker HM. Egg laying in *Aplysia*. II. Organization of central and peripheral pathways for initiating neurosecretory activity and behavioral patterns. *J Comp Physiol A* 164: 849–857, 1989.

Fisher T, Lin CH, Kaczmarek LK. The peptide FMRFa terminates a discharge in *Aplysia* bag cell neurons by modulating calcium, potassium, and chloride conductances. *J Neurophysiol* 69: 2164–2173, 1993.

Frazier WT, Kandel ER, Kupfermann I, Waziri R, Coggeshall RE. Morphological and functional properties of identified neurons in the abdominal ganglion of *Aplysia californica*. *J Neurophysiol* 30: 1288–1351, 1967.

Gardner P, Ogden DC, Colquhoun D. Conductances of single ion channels opened by nicotinic agonists are indistinguishable. *Nature* 309: 160–162, 1984.

Grassi F, Giovannelli A, Fucile S, Eusebi F. Activation of the nicotinic acetylcholine receptor mobilizes calcium from caffeine-insensitive stores in C2C12 mouse myotubes. *Pflügers Arch* 422: 591–598, 1993.

Groten CJ, Magoski NS. PKC enhances the capacity for secretion by rapidly recruiting covert voltage-gated Ca^{2+} channels to the membrane. *J Neurosci* 35: 2747–2765, 2015.

Gustafsson B, Galvan M, Grafe P, Wigstrom H. A transient outward current in a mammalian central neurone blocked by 4-aminopyridine. *Nature* 299: 252–254, 1982.

Hagiwara S, Saito N. Voltage-current relations in nerve cell membrane of *Onchidium verruculatum*. *J Physiol* 148: 161–179, 1959.

Hamon B, Glowinski J, Giaume C. Nicotine inhibits slowly inactivating K^+ currents in rat cultured striatal neurons. *Pflügers Arch* 434: 642–645, 1997.

Hermann A, Gorman AL. Effects of tetraethylammonium on potassium currents in a molluscan neurons. *J Gen Physiol* 78: 87–110, 1981.

Hille B. *Ionic Channels of Excitable Membranes*. Sunderland, MA: Sinauer, 2001.

Inoue M, Kuriyama H. Muscarinic receptor is coupled with a cation channel through a GTP-binding protein in guinea-pig chromaffin cells. *J Physiol* 436: 511–529, 1991.

Jennings KR, Kaczmarek LK, Hewick RM, Dreyer WJ, Strumwasser F. Protein phosphorylation during afterdischarge in peptidergic neurons of *Aplysia*. *J Neurosci* 2: 158–168, 1982.

Johnston J, Forsythe ID, Kopp-Scheinpflug C. Going native: voltage-gated potassium channels controlling neuronal excitability. *J Physiol* 588: 3187–3200, 2010.

Kaczmarek LK, Jennings KR, Strumwasser F, Nairn AC, Walter U, Wilson FD, Greengard P. Microinjection of catalytic subunit of cyclic AMP-dependent protein kinase enhances calcium action potentials in bag cell neurons in cell culture. *Proc Natl Acad Sci USA* 77: 7487–7491, 1980.

Kaczmarek LK, Jennings K, Strumwasser F. An early sodium and a late calcium phase in the afterdischarge of peptide-secreting neurons of *Aplysia*. *Brain Res* 238: 105–115, 1982.

Kaczmarek LK, Strumwasser F. A voltage-clamp analysis of currents in isolated peptidergic neurons of *Aplysia*. *J Neurophysiol* 52: 340–349, 1984.

Kehoe J. Three acetylcholine receptors in *Aplysia* neurones. *J Physiol* 225: 115–146, 1972.

Kehoe J. Glutamate activates a K^+ conductance increase in *Aplysia* neurons that appears to be independent of G-proteins. *Neuron* 13: 691–702, 1994.

Klein M, Kandel ER. Presynaptic modulation of voltage-dependent Ca^{2+} current: mechanism for behavioral sensitization in *Aplysia californica*. *Proc Natl Acad Sci USA* 75: 3512–3516, 1978.

Kupfermann I, Kandel ER. Electrophysiological properties and functional interconnections of two symmetrical neurosecretory clusters (bag cells) in abdominal ganglion of *Aplysia*. *J Neurophysiol* 33: 865–876, 1970.

Kupfermann I, Kandel ER, Coggeshall R. Synchronized activity in neurosecretory cell cluster in *Aplysia*. *Physiologist* 9: 223, 1966.

Langley JN. On the reaction of cells and of nerve-endings to certain poisons, chiefly as regards the reaction of striated muscle to nicotine and to curare. *J Physiol* 33: 374–413, 1905.

Lee YS, Choia SL, Lee SH, Kim H, Park H, Lee N, Lee SH, Chae YS, Jang DJ, Kandel ER, Kaang BK. Identification of a serotonin receptor coupled to adenylyl cyclase involved in learning-related heterosynaptic facilitation in *Aplysia*. *Proc Natl Acad Sci USA* 106: 14634–14639, 2009.

Lee RH, Heckman CJ. Bistability in spinal motoneurons in vivo: systematic variations in persistent inward currents. *J Neurophysiol* 80: 583–593, 1998.

Lemos JR, Levitan IB. Intracellular injection of guanyl nucleotides alters the serotonin-induced increase in potassium conductance in *Aplysia* neuron R15. *J Gen Physiol* 83: 269–285, 1984.

Levitan IB, Kaczmarek LK. *The Neuron: Cell and Molecular Biology*. New York: Oxford University Press, 2002.

Loechner KJ, Azhderian EM, Dreyer R, Kaczmarek LK. Progressive potentiation of peptide release during a neuronal discharge. *J Neurophysiol* 63: 738–744, 1990.

Lorente de Nó R. On the effect of certain quaternary ammonium ions upon frog nerve. *J Cell Comp Physiol* 33, Suppl: 167–231, 1949.

Lüthi A, Gähwiler BH, Gerber U. 1*S*,3*R*-ACPD induces a region of negative slope conductance in the steady-state current-voltage relationship of hippocampal pyramidal cells. *J Neurophysiol* 77: 221–228, 1997.

MacKinnon R, Yellen G. Mutations affecting TEA blockade and ion permeation in voltage-activated K^+ channels. *Science* 250: 276–279, 1990.

Magoski NS, Bauce LG, Syed NI, Bulloch AGM. Dopaminergic transmission between identified neurons from the mollusk, *Lymnaea stagnalis*. *J Neurophysiol* 74: 1287–1300, 1995.

Marrion NV, Smart TG, Marsh SJ, Brown DA. Muscarinic suppression of the M-current in the rat sympathetic ganglion is mediated by receptors of the M1-subtype. *Br J Pharmacol* 98: 557–573, 1989.

Mathie A, Al-Moubarak E, Veale EL. Gating of two pore domain potassium channels. *J Physiol* 588: 3149–3156, 2010.

Mayer B. How much nicotine kills a human? Tracing back the generally accepted lethal dose to dubious self-experiments in the nineteenth century. *Arch Toxicol* 88: 5–7, 2014.

McIntosh JM, Yoshikami D, Mahe E, Nielsen DB, Rivier JE, Gray WR, Olivera BM. A nicotinic acetylcholine-receptor ligand of unique specificity, alpha-conotoxin-ImI. *J Biol Chem* 269: 16733–16739, 1994.

Michel S, Wayne NL. Neurohormone secretion persists after post-afterdischarge membrane depolarization and cytosolic calcium elevation in peptidergic neurons in intact nervous tissue. *J Neurosci* 22: 9063–9069, 2002.

Neher E, Lux HD. Differential action of TEA^+ on two K^+-current components of a molluscan neurone. *Pflügers Arch* 336: 87–100, 1972.

Nick TA, Kaczmarek LK, Carew TJ. Ionic currents underlying developmental regulation of repetitive firing in *Aplysia* bag cell neurons. *J Neurosci* 16: 7583–7598, 1996a.

Nick TA, Moreira JE, Kaczmarek LK, Carew TJ, Wayne NL. Developmental dissociation of excitability and secretory ability in *Aplysia* bag cell neurons. *J Neurophysiol* 76: 3351–3359, 1996b.

Partridge LD, Thompson SH, Smith SJ, Connor JA. Current-voltage relationships of repetitively firing neurons. *Brain Res* 164: 69–79, 1979.

Piomelli D, Shapiro E, Feinmark SJ, Schwartz JH. Metabolites of arachidonic-acid in the nervous system of *Aplysia*. Possible mediators of synaptic modulation. *J Neurosci* 7: 3675–3686, 1987a.

Piomelli D, Volterra A, Dale N, Siegelbaum SA, Kandel ER, Schwartz JH, Belardetti F. Lipoxygenase metabolites of arachidonic-acid as second messengers for presynaptic inhibition of *Aplysia* sensory cells. *Nature* 328: 38–43, 1987b.

Quattrocki EA, Marshall J, Kaczmarek LK. A Shab potassium channel contributes to action potential broadening in peptidergic neurons. *Neuron* 12: 73–86, 1994.

Shen KZ, Johnson SW. Group I mGluRs evoke K-ATP current by intracellular Ca^{2+} mobilization in rat subthalamus neurons. *J Pharmacol Exp Ther* 345: 139–150, 2013.

Shuster MJ, Camardo JS, Siegelbaum SA, Kandel ER. Cyclic AMP-dependent protein kinase closes the serotonin-sensitive K^+ channels of *Aplysia* sensory neurones in cell-free membrane patches. *Nature* 313: 392–395, 1985.

Siegelbaum SA, Camardo JS, Kandel ER. Serotonin and cyclic AMP close single K^+ channels in *Aplysia* sensory neurones. *Nature* 299: 413–417, 1982.

Stone CA, Torchiana ML, Navarro A, Beyer KH. Ganglionic blocking properties of 3-methylaminoisocamphane hydrochloride (mecamylamine): a secondary amine. *J Pharmacol Exp Ther* 117: 169–183, 1956.

Strong JA. Modulation of potassium current kinetics in bag cell neurons of *Aplysia* by an activator of adenylate cyclase. *J Neurosci* 4: 2772–2783, 1984.

Strong JA, Kaczmarek LK. Multiple components of delayed potassium current in peptidergic neurons of *Aplysia*: modulation by an activator of adenylate cyclase. *J Neurosci* 6: 814–822, 1986.

Suzuki T, Hide I, Matsubara A, Hama C, Harada K, Miyano K, Andra M, Matsubayashi H, Sakai N, Kohsaka S, Inoue K, Nakata Y. Microglial alpha 7 nicotinic acetylcholine receptors drive a phospholipase C/IP_3 pathway and modulate the cell activation toward a neuroprotective role. *J Neurosci Res* 83: 1461–1470, 2006.

Tam AK, Gardam KE, Lamb S, Kachoei BA, Magoski NS. Role for protein kinase C in controlling *Aplysia* bag cell neuron excitability. *Neuroscience* 179: 41–55, 2011.

Tang G, Hanna ST, Wang R. Effects of nicotine on K^+ channel currents in vascular smooth muscle cells from rat tail arteries. *Eur J Pharmacol* 364: 247–254, 1999.

Thany SH, Courjaret R, Lapied B. Effect of calcium on nicotine-induced current expressed by an atypical alpha-bungarotoxin-insensitive nAChR2. *Neurosci Lett* 438: 317–321, 2008.

Tieman TL, Steel DL, Gor Y, Kehoe J, Schwartz JH, Feinmark SJ. A pertussis toxin-sensitive 8-lipoxygenase pathway is activated by a nicotinic acetylcholine receptor in *Aplysia* neurons. *J Neurophysiol* 85: 2150–2158, 2001.

Wang H, Shi H, Zhang L, Pourrier M, Yang B, Nattel S, Wang Z. Nicotine is a potent blocker of the cardiac A-type K^+ channels. Effects on cloned K_V43 channels and native transient outward current. *Circulation* 102: 1165–1171, 2000a.

Wang H, Yang B, Zhang L, Xu D, Wang Z. Direct block of inward rectifier potassium channels by nicotine. *Toxicol Appl Pharmacol* 164: 97–101, 2000b.

White SH, Magoski NS. Acetylcholine-evoked afterdischarge in *Aplysia* bag cell neurons. *J Neurophysiol* 107: 2672–2685, 2012.

White SH, Carter CJ, Magoski NS. A potentially novel nicotinic receptor in *Aplysia* neuroendocrine cells. *J Neurophysiol* 112: 446–462, 2014.

Wilson GF, Richardson FC, Fisher TE, Olivera BM, Kaczmarek LK. Identification and characterization of a Ca^{2+}-sensitive nonspecific cation channel underlying prolonged repetitive firing in *Aplysia* neurons. *J Neurosci* 16: 3661–3671, 1996.

Wilson WA, Wachtel H. Negative resistance characteristic essential for the maintenance of slow oscillations in bursting neurons. *Science* 186: 932–934, 1974.

Yang J, Ye M, Tian C, Yang M, Wang Y, Shu Y. Dopaminergic modulation of axonal potassium channels and action potential waveform in pyramidal neurons of prefrontal cortex. *J Physiol* 591: 3233–3251, 2013.

Zhang Y, Joiner WJ, Bhattacharjee A, Rassendren F, Magoski NS, Kaczmarek LK. The appearance of a protein kinase A-regulated splice isoform of slo is associated with the maturation of neurons that control reproductive behavior. *J Biol Chem* 279: 52324–52330, 2004.

Zhang Y, Kaczmarek LK. Bag cell neurons. *Scholarpedia J* 3: 4095, 2008.

Zhang Y, Magoski NS, Kaczmarek LK. Prolonged activation of Ca^{2+}-activated K^+ current contributes to the long-lasting refractory period of *Aplysia* bag cell neurons. *J Neurosci* 22: 10134–10141, 2002.